A scalable model for design and control of turboprop engines for advanced propulsion systems

Cite as: AIP Conference Proceedings **2191**, 020061 (2019); https://doi.org/10.1063/1.5138794
Published Online: 17 December 2019

C. L. De Pascalis, T. Donateo, and A. Ficarella

A Scalable Model for Design and Control of Turboprop Engines for Advanced Propulsion Systems

C. L. De Pascalis[1, b)], T. Donateo[1, a)], and A. Ficarella[1]

[1]*Dept. of Engineering for Innovation, University of Salento, Lecce, Italy*

[a)]*teresa.donateo@unisalento.it*
[b)]*claudia.depascalis@unisalento.it*

Abstract. In this study, a methodology is proposed for designing turboprop engines and evaluating their off-design performance. It involves optimization steps for the choice of some of the system design parameters and adaptive scaling methods for the turbomachinery and propeller maps. Results show that it leads to a good estimation of the performance of the real architecture of the existing aircraft and is suitable to be used for innovative application such as the sizing of the engine for advanced propulsion systems like the hybrid-electric architectures with increasing hybridization factor.

INTRODUCTION

In the years, a more and more increasing interest has been earned by new concepts of aircraft propulsion that involve the introduction of electrification [1]. Fletcher et al. [2] summarized the advantages of hybrid electric aircraft (improved efficiency at part load, use of excess power generation for auxiliaries, etc.) and put into evidence that the one of the most significant benefits is the flexibility in configuration and operation. The introduction of electric and hybrid-electric technology has drastically opened the design space thanks to the synergy with distributed propulsion and Boundary Layer Ingestion [3]. Besides the proved benefits that electrical devices can bring in terms of environmental impact, there are obstacles regarding battery technologies mainly, in particular about their specific energy and power. While waiting for the improvements in batteries, it is interesting to investigate the performance of hybrid electric power systems with today technology by means of numerical methods and optimization tools that can allow exploiting the advantages of hybridization through energy management, integration, multi-functionalization, distributed propulsion, etc. [4]. To this scope, a comprehensive simulation/optimization methodology was proposed in previous investigations of some of the authors [5] to parallel and series hybrid electric configurations using either positive displacements engines or fuel cell as fuel converter.

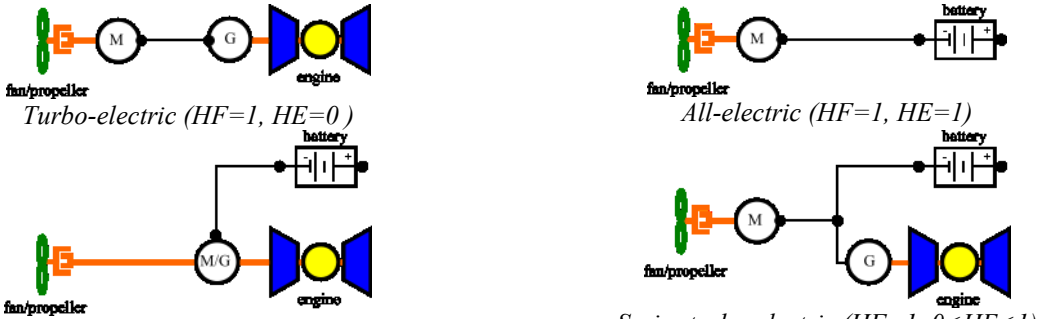

FIGURE 1. Electrification schemes

74th ATI National Congress
AIP Conf. Proc. 2191, 020061-1–020061-10; https://doi.org/10.1063/1.5138794
Published by AIP Publishing. 978-0-7354-1938-4/$30.00

While the hybridization of piston-propelled airplanes uses almost the same schemes, simulation approach and energy management techniques of the automotive field [6,7,8], the hybridization of turboshaft and turboprop engines requires a completely new approach because the engine needs to be completely redesigned [9-11]. The most common electrification schemes for large aircraft are shown in **FIGURE 1**. Note that the turboelectric configuration does not involve the usage of batteries as secondary storage system but decouples the production of the mechanical power (gas turbine shaft) from the generation of the thrust through one or more propellers or fans, thus allowing distributed propulsions. For a more complete description and comparison, it could be useful to refer to a recent review performed by Brelje and Martins [12].

The architectures of **FIGURE 1** can be described in terms of power and energy hybridization factors 11]. The power hybridization factor is defined as:

$$HF = \frac{P_{EM}}{P_{TOT}} = \frac{P_{EM}}{P_{ICE} + P_{EM}} \tag{1}$$

where P_{EM} is the power delivered by the motor, P_{ICE} is the power from the engine, and P_{TOT} is the total mechanical power transferred to the propeller shaft by the hybrid power system.

The energy hybridization factor HE is defined as:

$$HE = \frac{E_{batt}}{E_{batt} + E_{fuel}} \tag{2}$$

where E_{batt} is the energy stored in the battery, E_{fuel} is the energy content of the fuel tank.

This investigation aims at developing a model to be used for the design and performance analysis of turbo-prop engines in architectures with increasing HF through an "adaptive scalable model". The paper consists of three parts. It starts with the description of the proposed "adaptive scalable model". Then, the overall optimization process for the choice of the optimal design is described and applied to a conventional turboprop engine (HE=0 and HF=0) in terms of equivalent brake specific fuel consumption (EBSFC) and payload weight. The last section performs the sizing of thermal engine and electric machine in a parallel hybrid-electric configuration with HF ranging from 0 to 0.6. Note that HE is not considered here because the sizing of the battery is not considered in this paper. However, the proposed methodology for the design of turboshaft engines can be easily included in the overall design of a hybrid power system [5].

SCALABILITY MODEL

Scalability is here meant as the possibility to obtain a good estimation of the behavior of an energy device starting form data of a reference device with the same technology but different size. The size of the new engine with respect to the reference one is expressed in terms of scaling factors (S.F.) that are used to build the new (or modified) map for each component of the engine. The scaling method here proposed (**FIGURE 2**) uses the library of compressors and turbines available in the well-known commercial software Gas-turbine Simulation Program (GSP)[13], and is based on the standard scaling procedure described in[14] but with an innovative approach that we will call "adaptive scaling".

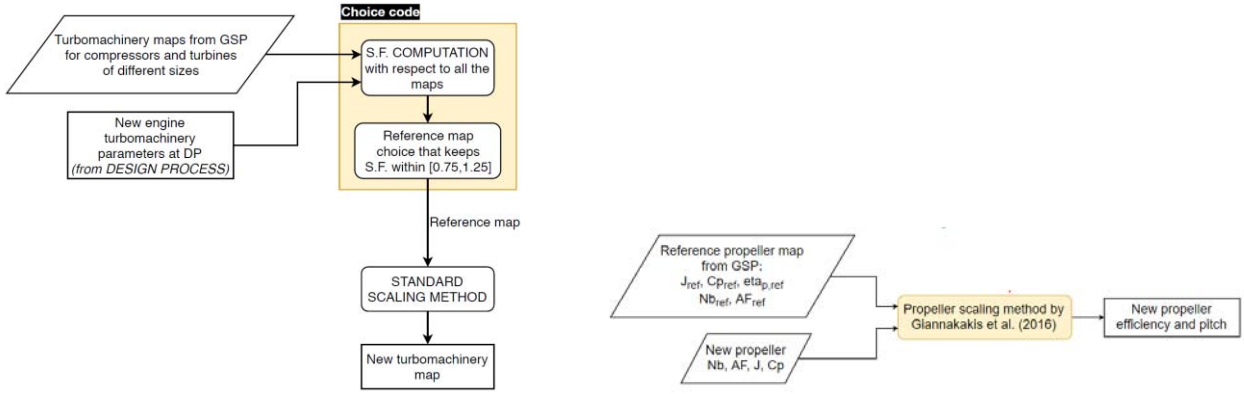

a. b.

FIGURE 2. The adaptive scaling method

In fact, the standard scaling technique is known to return accurate results only when the scaling factor is around 1 so that the reference component and new one have similar size. In the years, more complex scaling strategies have been presented in literature (see for example [14]), but the lack of available data in the aeronautical field makes them often unusable. This problem is addressed here by adaptively changing the reference map in order to keep the S.F. between 0.75 and 1.25. The block that performs this procedure is called "Choice code" in the flowchart of **FIGURE 2**.

As for the propeller map, the authors selected the scaling method proposed by Giannakakis et al. (2016) [15]. In the computation of the scaled parameters, it takes into account the induced velocity and viscous losses of the new devices, which differ from the reference propeller.

OPTIMIZATION OF A CONVENTIONAL TURBOPROP ENGINE

The design of the engine is performed with the procedure described in **FIGURE *3***. The aircraft mission profile is used as input to compute the propulsive power request at each phase of the flight by using the balance of the forces acting on the plane ("AERODYNAMICS" block). Then, based on the design-point (DP) conditions, the turbo-gas engine is designed ("TURBO-GAS DESIGN" block). This block returns the specifications of the engine and the amount of power to be delivered by the propeller at DP which is used to size the propeller ("PROPELLER DESIGN" block). After defining the size and the DP-parameters of the engine, an OFF-DESIGN ANALYSIS is performed (**FIGURE 3**b).

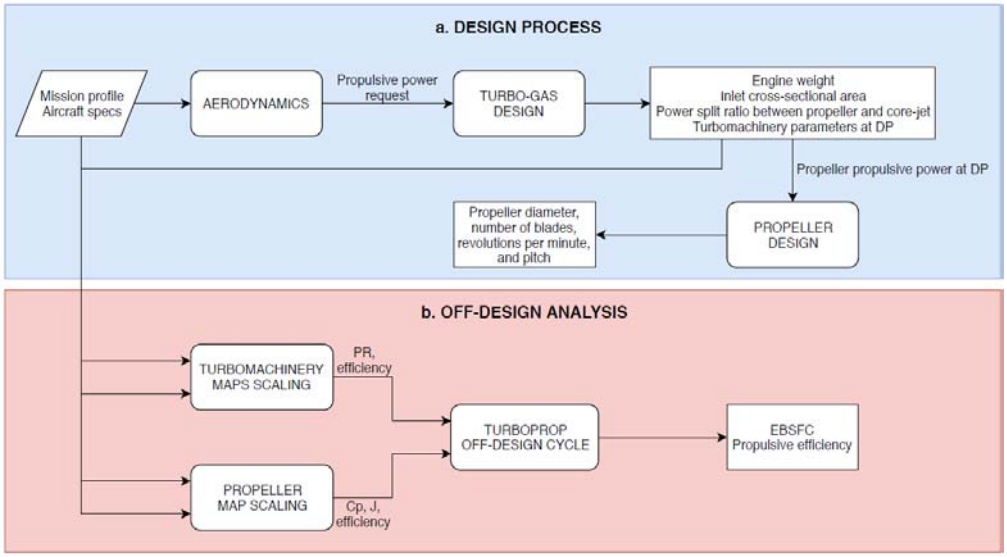

FIGURE 3. The turboprop model flowchart

The "TURBO-GAS DESIGN" block

The details of the "TURBO-GAS DESIGN" block are explained in **FIGURE 4**. A database of existing turboprop engines [16] is considered in order to select the technology (called reference technology) with the propulsive power nearest to the output of the "AERODYNAMICS" block. Then, the overall pressure ratio (OPR) and the mass flow rate at the inlet entrance (m_0) of the selected device are taken as reference values for the subsequent computations. The reference value for the maximum total temperature at the burner exit is chosen on the basis of the materials technologies considered for the new engine.

The evolutionary optimization algorithm called SMS-EMOA (S-Metric Selection Evolutionary Multi-Objective Algorithm) [17] is used to optimize the design variables that are reported in **TABLE 1** together with their bounding values. During the optimization, the conventional thermodynamic cycle of a turbo-gas engine is considered to obtain the equivalent break specific fuel consumption (EBSFC, to be minimized) and the propulsive efficiency (η_p to be maximized).

TABLE *2* reports the assumptions for the thermodynamic cycle at DP. Note that the model considers only a constant number of spools (two) in the present version, but will be extended to different configurations as future development. The optimization procedure also checks that the power request is satisfied by means of a constraint.

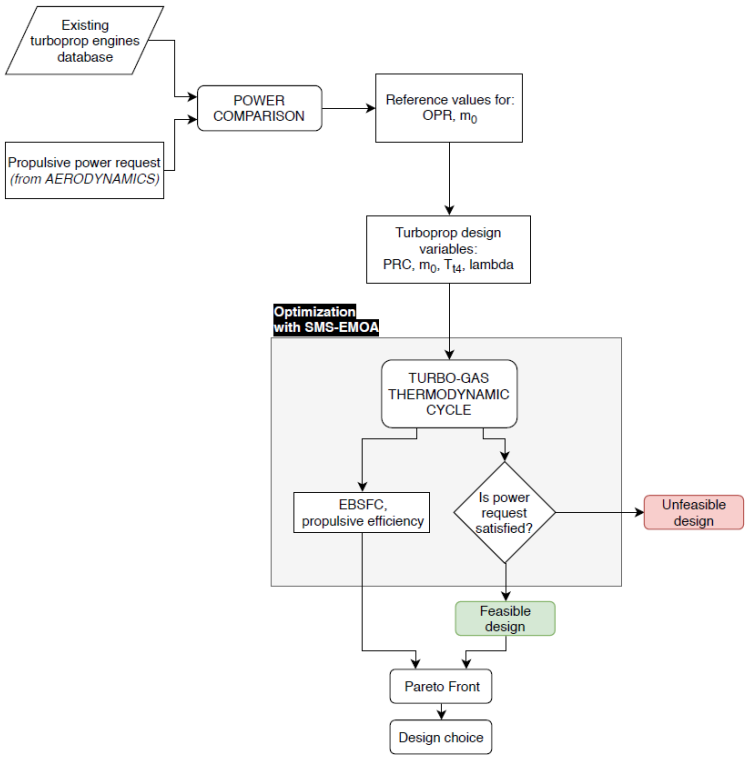

FIGURE 4. Flowchart of "TURBO-GAS DESIGN"

TABLE 1. Turbo-gas design variables

Design variable	Mean value	Delta
Compressor pressure ratio (PR_C)	OPR of the selected technology from the database	30%
Power split ratio between propeller and jet-flow (λ)	0.85	0.10
Air mass flow rate at inlet entrance (m_0)	m_0 of the selected technology from the database	30%
Maximum temperature at the turbine entrance (Tt_4)	Based on the material technology	10%

TABLE 2. Assumptions for the thermodynamic cycle at DP

Parameter	$\eta_{d,is}$	η_c	η_b	PR_b	η_t	$\eta_{n,is}$	η_m	η_{prop}
Value	0.97	0.821	0.985	0.94	0.85	0.98	0.98	0.65

The "PROPELLER DESIGN" block

A second optimization with SMS-EMOA is performed in order to find the optimal set of the design variables of the propeller (**TABLE 3**) that maximizes its efficiency. The optimization process takes as input the propeller map from GSP software to be considered as reference, the propulsive power to be delivered by the propeller, and the flight Mach-number at the design point and computes the new (or scaled) propeller-map through the model of **FIGURE 2**b for each set of values of the design variables (J, Cp, Nb, and AF). Then, the efficiency and the propeller blades pitch (Bp) are derived from the new map while the propeller diameter is calculated as follows:

$$P_{ax,prop} = \frac{P_{p,prop}}{\eta_{prop}} \tag{3}$$

$$D_{prop} = \sqrt{\frac{J^3 \cdot P_{ax,prop}}{\rho \cdot V^3 \cdot C_p}}$$

$$n_{prop} = \frac{60 \cdot V}{J \cdot D_{prop}}$$

TABLE 3 shows the design variables of the propeller, together with their upper and lower limits.

TABLE 3. Propeller design variables

Design variable	Min value	Max value
Advance ratio (J) @ design point	0.5	4
Propeller coefficient (Cp) @ design point	0.01	4
Number of blades (Nb)	2	6
Affecting factor (AF)	100	500

Off-design Analysis

The input data of the off-design analysis, described in **FIGURE 5**, are:

- The flight conditions (free-stream air pressure, temperature, and Mach number);
- The specification of the turbo-gas and the propeller from the design procedure;
- Some parameters assumed to be constant and listed in **TABLE 4**.

Other assumptions and initializations are reported in the yellow rectangle of **FIGURE 5**.

TABLE 4. Constant parameters for the off-design analysis

Parameter	η_d	η_b	PR_b	η_m	η_n
Value	0.97	0.985	0.94	0.98	0.98

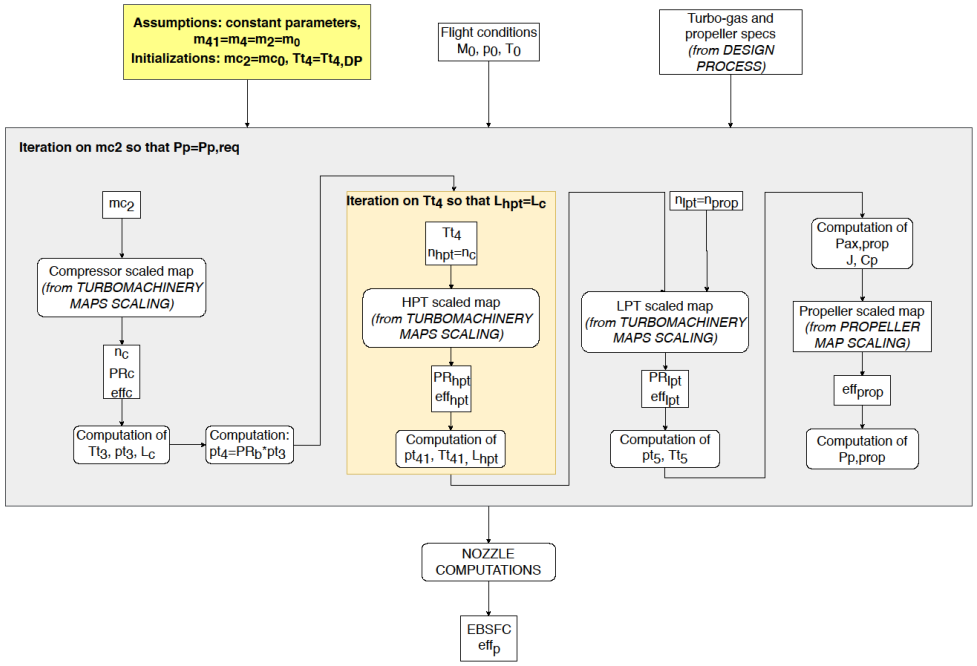

FIGURE 5. Flowchart of the Off-design analysis

An iteration is run for the evaluation of the corrected mass flow rate at the entrance of the compressor (mc_2), so that the propulsive power delivered by the propeller matches the required power. Then, the turbo-gas thermodynamic cycle simulated with the turbomachinery and propeller maps found in the design process. Within the thermodynamic cycle, a second iteration is performed for the temperature at the entrance of the high-pressure turbine (Tt_4), in order to equal, in absolute value, the shaft power of turbine and compressor. The results of the off-design analysis are the scaled maps, the corrected mass flow rate at the entrance of compressor and turbines, the Equivalent Brake Specific Fuel Consumption (EBSFC) and the propulsive efficiency at the considered off-design point.

Validation of the procedure

The "Turbo-Gas Design" procedure is here applied, for validation, to the ATR 72-600. The selected design points (DP) are take-off for the sizing and cruise for the off-design analysis (**TABLE 5**).

TABLE 5. Input parameters for the validation[18]

	Take-off (DP)	Cruise (off-design)
P_{prop} [MW]	2.05	1.17
M_0	0.176	0.46
Z_0 [m]	0	7315

The optimization for the design process (see ***TABLE 1***) was run with the following reference values: PRC= 13.2, m_0 =12.3 kg/s and Tt4 = 1100K. The maps found with the adaptive scaling procedure are shown in **Figure 6**, where PR is the pressure ratio, Wc the corrected mass-flow rate, and Nc the normalized value of the corrected number of revolutions per minute.

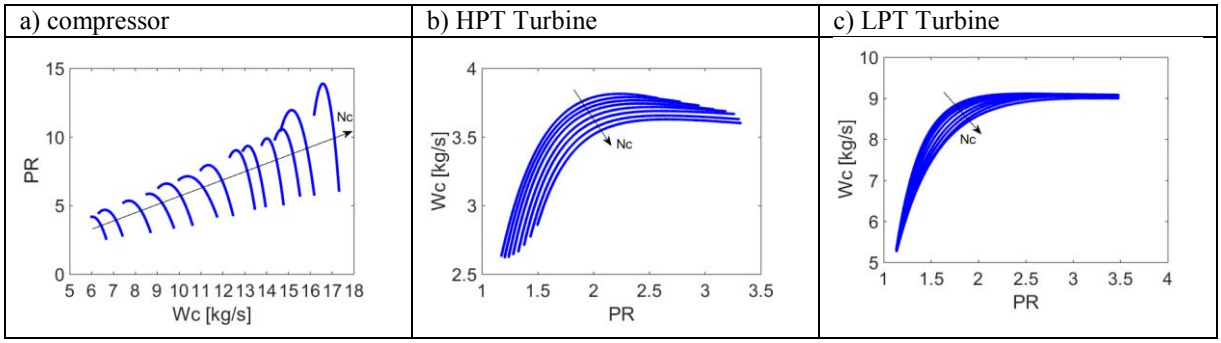

FIGURE 6 Maps of the engine components found with the adaptive scaling procedure

TABLE *6* shows the comparison between the specifications of the actual engine of the ATR 72-600 (PW127M) and the input and output parameters of the optimal solution found in this study. Parameter λ is considered to be the same for all flight phases. The comparison is done both at take-off (DP) and cruise (off-design) conditions.
It is possible to observe that the proposed method reaches a good estimation of the performance of the actual architecture at the best of the authors' knowledge. Other parameters not available in literature for the PW127M engine (reported as N.A. in **TABLE 6**) still show realistic values in the optimal design from this study.
It is important to underline some critical aspects in the choice of Tt_4. During several repetitions of the computations, it was observed that the optimization moved always towards the maximum value of Tt_4 that sensibly affects the optimal values of the other parameters, as **FIGURE 7** shows, thus the engine performance.
For this reason, the choice of its range is of particular importance for the optimization and depends on the material technology considered for the new engine. Since the intent of this section is the validation of the model, the authors considered the value reported for Tt_4 in TABLE 6 after checking the actual range of the temperature limits of the PW100's engines family [19, 20]. Due to the relevant influence of Tt_4 in the engine sizing, an iteration loop on its mean value is used. The temperature is increased by 50 [K] at each iteration from the initial value of 1100 [K] if no

feasible solutions are found by the optimization problem within the range of 1100 K ± 10%. This will be critical in the second section of this paper, where different sizes of the engine are designed and investigated.

TABLE 6. Performance comparison for the turbo-gas model validation

DESIGN POINT (take-off)				**OFF-DESIGN ANALYSIS (cruise)**			
PRC	9.24	N.A.	-	PRC	9.61	N.A.	-
λ	0.88	N.A.	-	η_c	0.82	N.A	-
Tt_4 [K]	1210	up to 1073 @ SL *	[19]	Tt_4 [K]	1391	up to 1073 @ SL *	[19]
m_0 [kg/s]	15.6	~16.0	[21]	m_0 [kg/s]	6.63	N.A.	-
m_f [kg/s]	0.30	N.A.	-	m_f [kg/s]	0.174	0.212	[18]
PR_{hpt}	2.80	N.A.	-	PR_{hpt}	2.55	N.A.	-
PR_{lpt}	3.11	N.A.	-	PR_{lpt}	2.92	N.A.	-
mc_4 [kg/s]	3.61	N.A.	-	mc_4 [kg/s]	3.61	N.A.	-
mc_{41} [kg/s]	8.88	N.A.	-	mc_{41} [kg/s]	9.57	N.A.	-
EBSFC [kg/kW/hr]	0.351	0.273	[22]	η_{hpt}	0.84	N.A	-
η_p	0.65	N.A.	-	η_{lpt}	0.62	N.A	-
M_{tp} [kg]	423.2	481.7	[19]	EBSFC [kg/kW/hr]	0.456	N.A.	-
				η_p	0.86	N.A.	-

* it can vary with the ambient temperature (another source [20] reports values between 1422 – 1533 [K] for the PW100's engines family)

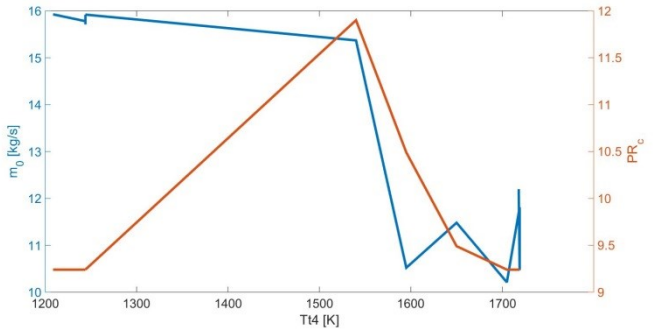

FIGURE 7. Analysis of the turbine inlet temperatureTt4

The "Propeller Design" procedure is also validated by considering the ATR 72-600 engine propeller, which is an Hamilton Standard 568F [18]. In this case, the cruise phase is considered as design point, because it is the longest mission segment along which the device has to guarantee the highest efficiency. The input parameters are the propulsive power request of a single engine at cruise (0.7 MW) and the Mach number (0.43). The model returns the values reported in **TABLE 7**. Again, a good estimation of the performance of the actual architecture is obtained at the best of the authors' knowledge.

TABLE 7. Performance comparison for the propeller model validation

DESIGN POINT (cruise)			
J	2.21	N.A.	-
Cp	0.33	N.A.	-
Nblades	6	6	[18]
AF	238.5	N.A.	-
η_{prop}	0.899	N.A.	-
B_{prop}		N.A.	-
D_{prop} [m]	3.91	3.93	[18]
n_{prop} [rpm]	994.0	N.A.	-

SIZING A HYBRID ELECTRIC TURBOPROP ENGINE

In this section, the design of the turboprop engine is performed in the framework of a parallel hybrid electric configuration with a power hybridization factor (Eq. (1)) ranging between 0 and 0.6 with a step of 0.1 The ATR 72-600 aircraft is considered again as reference and the engine power is reduced from 2.05 MW at HF=0 (full-thermal configuration of **TABLE 5**) to 0.82 MW at HF=0.6.

$$P_{tp} = [1 - \mathrm{HF}] \cdot P_{p,DP} \tag{4}$$

where P_{tp} is the turboprop engine power and $P_{p,DP}$ is the total propulsive power required at DP, i.e. 2.05 MW.

The results are presented in **FIGURE 8** and **FIGURE 9**, which show the different sizing of the two converters (in terms of both power and weight) and the corresponding design variables, respectively. A power-to-weight ratio of 3 kW/kg is assumed as representative of today electric machines for aircraft propulsion.

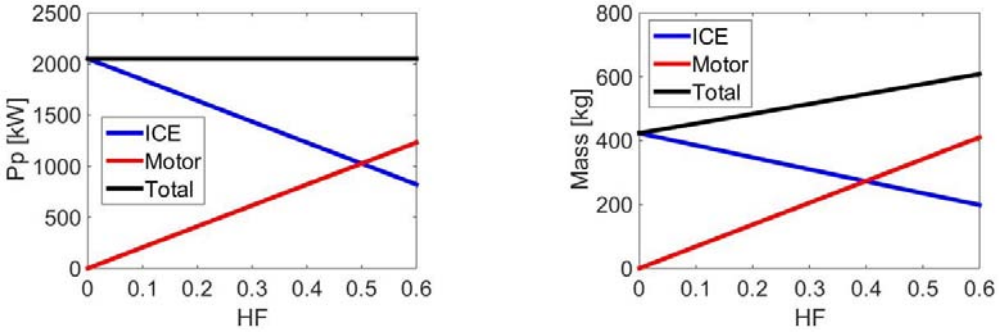

FIGURE 8. Contribution of engine and motor to total power and mass as a function of the hybridization ratio

The trends of the design variables are reported in blue in **FIGURE 9**, while the parameters resulting from the thermodynamic model are shown in red. Note that the design parameters (PRc, Tt4, m0, and lambda or λ) adjust themselves in order to obtain a value of the propulsive efficiency that is the same for the optimal designs and equal to 0.65. In particular, m_0 tends to decrease when HR increases, showing a strong reduction from HF=0 to HF=0.1 that also corresponds to an important rising of Tt_4. Then, for HF>0.1, Tt_4 decreases with HF while m_0 has a plateau. The same trend of Tt_4 is also followed by the air-to-fuel ratio "f", except for the segment between HF=0.2 and HF=0.3 where it increases while Tt4 decreases. On the contrary, EBSFC shows a mirrored behavior with respect to PR_C that has a steep rise between HF=0.2 and HF=0.3, probably influencing the trend of "f" described above, with a net differentiation of its value with respect to the value of the full-thermal case. Finally, in the hybrid configurations, lambda (λ) is always higher than the conventional case, and shows the steepest increase between HF=0 and HF=0.1.

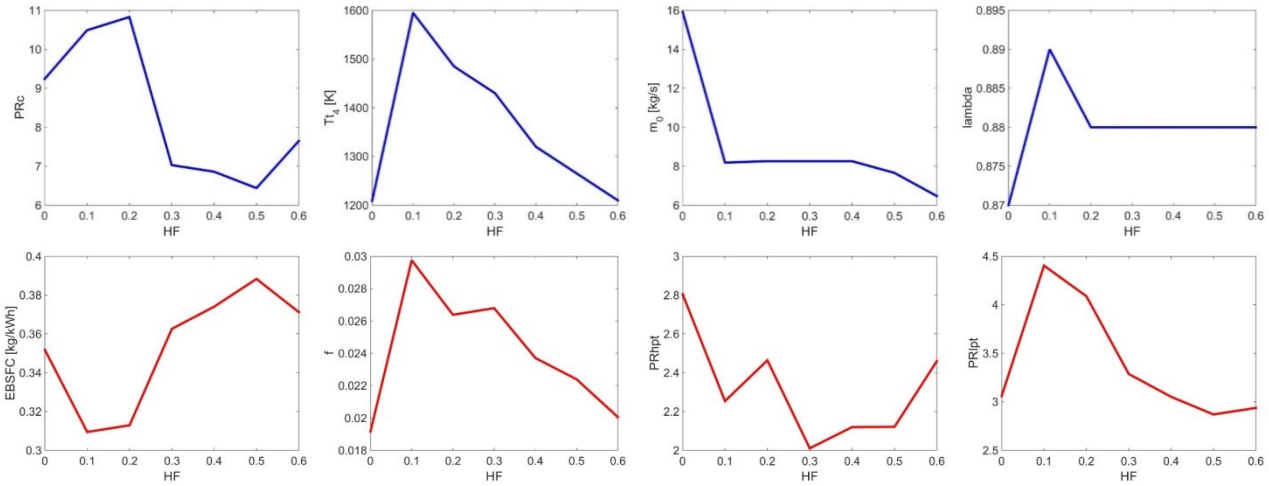

FIGURE 9. Design variables and objective functions of the different configurations, plus other resulting parameters

It is interesting to understand what happens between HF=0 and HF=0.1, where most of the parameters analyzed above (Tt4, m0, lambda, f) shows an evident variation with respect to the baseline case (HF=0).
FIGURE 10 shows a comparison between the nominal power of the "reference technology" (from the turboprop engines database) and the target power of the engine. It is possible to observe that between HF=0 and HF=0.1 there is a net reduction of the reference power, which at HF=0.1 is farthest from the required value. This explains the strong increase of Tt4 needed to make up for the not-well-centered mean value of the other design variables. Most likely, a wider database can keep lower this difference and lead to best solutions.

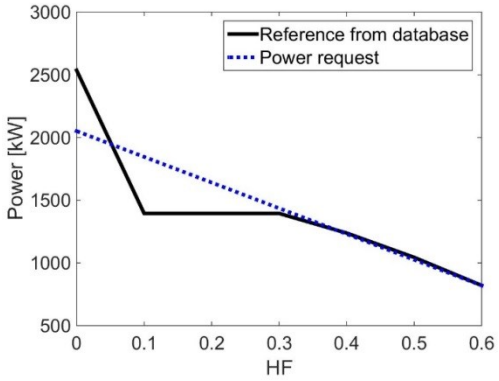

FIGURE 10. Power of the reference technology from the turboprop engines database vs power request

CONCLUSIONS

In this study, a methodology is proposed for the design and off-design analysis of a conventional turboprop engine based on the power request. It includes optimization steps for the choice of the design parameters and adaptive scaling methods for turbomachinery and propeller maps. The method is thought to be implemented in more complex simulation-codes for different purposes, such as the development of control strategies for the hybrid electric propulsion, which will be treated in the future developments. Here, the design method is also used to size a turboprop as a part of parallel hybrid electric power systems with increasing degree of hybridization. The methodology was applied ATR 72-600 regional aircraft as test case. The results show that the proposed methodology leads to a good estimation of the performance of the existing architecture of the ATR 72-600 and is suitable to be used for innovative application such as the sizing of the engine in hybrid-electric architectures. Future developments will involve the sizing of the whole power system including batteries based on the target mission profile of the aircraft.

Nomenclature

PR_C	Compressor pressure ratio	η_b	Burner efficiency
λ (or lambda)	Jump of enthalpy repartition between propeller and jet-flow	PR_b	Burner pneumatic efficiency
Tt_4 [K]	TIT (turbine inlet temperature)	η_t	Turbines efficiency: $()_{hpt}$ and $()_{lpt}$
m_0	Air mass flow	η_n	Nozzle efficiency
m_f	Fuel mass flow	η_m	Mechanical efficiency
f	Air-to-fuel ratio	η_{prop}	Propeller efficiency
PR_{hpt}	High pressure turbine (hpt) pressure ratio	$()_{is}$	Isentropic
PR_{lpt}	Low pressure turbine (lpt) pressure ratio	J	Propeller advance ratio
mc_4	Corrected mass flow at the HPT inlet	Cp	Propeller coefficient
mc_{41}	Corrected mass flow at the LPT inlet	Nb	Number of propeller blades
EBSFC	Equivalent brake specific fuel consumption	AF	Propeller affecting factor
η_p	Propulsive efficiency	M_0	Flight Mach number
M_{tp}	Turboprop engine mass	Z_0	Flight altitude
$\eta_{d,is}$	Inlet isentropic efficiency	$P_{p,req}$	Propulsive power request

η_c	Compressor efficiency	P_p	Engine Propulsive power
		SL	Sea Level conditions

REFERENCES

1. Abdul Sathar Eqbal, M.; Fernando, N.; Marino, M.; Wild, G. Hybrid Propulsion Systems for Remotely Piloted Aircraft Systems. *Aerospace* **2018**, *5*, 34.
2. Fletcher, S., Flynn, M.C., Jones, C.E. and Norman, P.J., Hybrid electric aircraft: State of the art and key electrical system challenges, IEEE Transportation Electrification eNewsletter, September 2016.
3. Gladin, J.C., Trawick, D., Perullo, C., Tai, J.C. and Mavris, D.N., Modeling and design of a partially electric distributed aircraft propulsion system with GT-HEAT, 55th AIAA Aerospace Sciences Meeting, AIAA SciTech Forum, (AIAA 2017-1924), 2017.
4. Donateo, T.; De Pascalis, C.L.; Ficarella, A. Synergy Effects in Electric and Hybrid Electric Aircraft. Aerospace 2019, 6, 32.
5. Donateo T, A Ficarella, Spedicato L., A method to analyze and optimize hybrid electric architectures applied to unmanned aerial vehicles, **Aircraft Engineering and Aerospace Technology**, Vol. 90 Issue: 5, pp.828-842, https://doi.org/10.1108/AEAT-11-2016-0202T, 2018.
6. Merical, K., Beechner, T. and Yelvington, P., Hybrid electric, heavy-fuel propulsion system for small unmanned aircraft", SAE Technical paper, 2014-01-2222, 2014.
7. Harmon, F.H., Conceptual design and simulation of a small hybrid-electric unmanned aerial vehicle, Journal of Aircraft, Vol. 43No. 5, 2006.
8. Donateo, T.; Totaro, R., Hybridization of training aircraft with real world flight profiles", Aircraft Engineering and Aerospace Technology, Vol. 91 Issue: 2, pp.353-365, https://doi.org/10.1108/AEAT-01-2018-0036, 2018
9. Bradley, M. and Droney, C., Subsonic ultra green aircraft research: phase I final report, NASA/CR-2011-216847, 2011.
10. Perullo, C., Trawick, D., Clifton, W., Urcinas, A., Tai, J. and Mavris, D. Development of a suite of hybrid electric propulsion modeling elements using NPSS, Proceedings of ASME Turbo Expo 2014, GT2014-27047, Dusseldorf, 2014.
11. Pornet, C. and Isikveren, A.T., Conceptual design of hybrid-electric transport aircraft, Progress in Aerospace Sciences, Vol. 79, pp. 114-135, doi: http://dx. doi.org/10.1016/j.paerosci.2015.09.002, 2015.
12. Brelje B.J., Martins J. R.R.A., Electric, Hybrid, and turboelectric fixed-win aircraft: A review of concepts, models and design approaches, Progress in Aerospace Sciences, vol. 104, pp 1-19, 2019.
13. https://www.gspteam.com/ last visit: May 15, 2019.
14. Kong, C.; Ki, J.; Kang, M. A New Scaling Method for Component Maps of Gas Turbine Using System Identification. In Journal of Engineering for Gas Turbines and Power, October 2003.
15. Giannakakis, P.; Goulos, I.; Laskaridis, P.; Pilidis, P. Novel Propeller Map Scaling Method. In Journal of propulsion and power, June 2016.
16. http://jet-engine.net/ last visit: May 30, 2019.
17. Emmerich, M.; Beume, N.; Naujoks, B. An EMO Algorithm Using the Hypervolume Measure as Selection Criterion. In Proceedings of the Third International Conference of Evolutionary Multi-Criterion Optimization EMO 2005, Guanajuato, Mexico, 9–11 March 2005.
18. http://www.atraircraft.com/products_app/media/pdf/Fiche_72-600_Juin-2014.pdf (accessed on June 09, 2019).
19. European Aviation Safety Agency EASA. Type-Certificate Data Sheet. No. IM.E.041for Engine PW100 series engines. Type Certificate Holder: Pratt & Whitney Canada. 1000 Marie-Victorin, Longueuil Quebec, J4G 1A1, Canada.
20. http://docplayer.net/47586006-The-market-for-aviation-turboprop-engines.html (accessed on June 09, 2019).
21. Filippone, A. (2012). Advanced Aircraft Flight Performance. New York, NY 10013-2473, USA: Cambridge University Press.
22. E. Hosking et al. The PWlOO Engine: 20 Years of Gas Turbine Technology Evolution. RTO AVT Symposium. Pratt und Whitney Canada Inc., 1998.